Formation Mechanism of the Ga₁₃ Keggin Ion: A Combined EXAFS and NMR Study

**Laurent J. Michot,*,† Emmanuelle Montargès-Pelletier,† Bruno S. Lartiges,†
Jean-Baptiste d'Espinose de la Caillerie,‡ and Valérie Briois§**

*Contribution from the Laboratoire Environnement et Minéralurgie INPL-ENSG-CNRS UMR 7569, BP 40,
54501 Vandoeuvre Cedex, France, Laboratoire de Physique Quantique CNRS ESA 7069, ESPCI,
10 rue Vauquelin, 75231 Paris Cedex 05, France, and Laboratoire pour l'Utilisation du Rayonnement
Electromagnétique Bât 209D Centre Universitaire Paris-Sud B.P. 34-91898 Orsay Cedex, France*

Abstract: The base hydrolysis of gallium chloride and gallium nitrate was followed by combining ⁷¹Ga NMR and Ga K-edge X-ray absorption spectroscopy measurements. Using such an approach, it can be shown unambiguously that the solution contains various trimeric and tetrameric species in the early hydrolytic stages before the formation of the Ga₁₃ polycation. This Keggin-type structure would then form by condensation of trimers and tetramers in disagreement with all of the previously published models that assume the existence of a monomer either tetrahedral or octahedral. In view of the parallel behavior of aluminum and gallium, this work can certainly be used to reach a better understanding of the hydrolytic chemistry of aluminum. This is of prime importance regarding the crucial role of this metal in natural systems and its widespread use as a coagulant in water treatment operations.

Introduction

Most metal cations undergo hydrolysis in aqueous solutions and, as stated by Baes and Messmer,[1] exhibit a "bewildering variety of behavior". Indeed, the combination of hydrolysis and condensation reactions in the aqueous medium leads, before the precipitation of the metal oxide or hydroxide, to the formation of numerous oligomeric or polymeric complexes with various structures.[2−5] A clear identification of the structure of the solute condensed species and of their evolution upon changes in the solution parameters (pH, temperature, concentration, influence of the anion...) is of crucial importance for understanding geocycling of hydrolyzing cations in natural aquatic environments. It is also required for improving water clarification by coagulation−flocculation techniques based on the use of hydrolyzed Fe(III) or Al(III) salts. Indeed, structure and charge of the hydrolysis products will control to a large extent, adsorption,[6−8] oxidation,[9] and coagulation[10] phenomena.

Among metals, aluminum and gallium present a distinct hydrolytic behavior. Indeed, it is the only two proven cases in which base hydrolysis leads, in a given pH/concentration range, to a Keggin-type polycation formed with 13 atoms. In the case of aluminum, this structure with 12 edge-linked octahedra surrounding a central tetrahedron atom was first evidenced by Johansson and co-workers[11−14] in the 1960s. Subsequent ²⁷Al NMR and SAXS studies[15−21] unambiguously revealed the presence of this polycation in base-hydrolyzed solutions of aluminum chloride and aluminum nitrate. In the case of gallium, potentiometric titration and ⁷¹Ga NMR experiments[22−24] have revealed that aluminum and gallium have a parallel hydrolytic behavior. Furthermore, clay intercalation experiments using hydrolyzed gallium chloride solutions[22,24,25−28] confirmed the

† LEM (INPL-ENSG-CNRS).
‡ LPQ (CNRS).
§ LURE (Universitaire Paris).
(1) Baes, C. F., Jr.; Mesmer, R. E. *The Hydrolysis of Cations*; Wiley: New York, 1976.
(2) Henry, M.; Jolivet, J. P.; Livage, J. *Struct. Bond.* **1992**, *77*, 153.
(3) Jolivet, J. P. *From Solution to Oxide. Cations Condensation in Aqueous Solution. Oxide Surface Chemistry.* [*De la solution à l'oxyde. Condensation des cations en solution aqueuse. Chimie de surface des oxydes.* Savoirs actuels.] InterEditions, CNRS Editions: Paris, 1994; pp 58−111.
(4) Livage, J.; Henry, M.; Jolivet, J. P. In *Multifunctional Mesoporous Inorganic Solids*; Sequeira, C. A. C., Hudson, M. J., Eds.; NATO Advanced Study Institute Series C400; Kluwer: Boston, 1993; pp 321−338.
(5) Richens, D. T. *The Chemistry of Aqua Ions. Synthesis, structure and reactivity. A tour through the periodic table of the elements;* John Wiley and Sons: New York, 1997.
(6) James, R. O.; Healy, T. W *J. Colloid Interface Sci.* **1972**, *40*, 42.
(7) James, R. O.; Stiglich, P. J.; Healy, T. W. *Faraday Discuss. Chem. Soc.* **1975**, *59*, 142.
(8) Crawford, R.; Harding, I. H.; Mainwaring, D. E. In *Surfaces of nanoparticles and porous materials;* Schwarz, J. A., Contescu, C. I., Eds.; Surfactant Science Series; Marcel Dekker: New York, 1997; Vol. 78, pp 675−710.
(9) Stumm, W. *Chemistry of the Solid-Water Interface*; John Wiley and Sons: New York, 1992.

(10) Lartiges, B. S.; Bottero, J. Y.; Derrendinger, L. S.; Humbert, B.; Tekely, P.; Suty, H. *Langmuir* **1997**, *13*, 142.
(11) Johansson, G. *Acta Chem. Scand.* **1960**, *14*, 771.
(12) Johansson, G.; Lundgren, G.; Sillén, L. G.; Söderquist, R. *Acta Chem. Scand.* **1960**, *14*, 769.
(13) Johansson, G. *Acta Chem. Scand.* **1962**, *16*, 403.
(14) Johansson, G. *Ark. Kemi.* **1963**, *21*, 321.
(15) Akitt, J. W.; Farthing, A. *J. Magn. Reson.* **1978**, *32*, 345.
(16) Akitt, J. W.; Mann, B. E. *J. Magn. Reson.* **1981**, *44*, 584.
(17) Akitt, J. W.; Farthing, A. *J. Chem. Soc., Dalton Trans.* **1981**, 1617.
(18) Akitt, J. W.; Elders, J. M. *J. Chem. Soc., Dalton Trans.* **1988**, 1347.
(19) Bottero, J. Y.; Cases, J. M.; Fiessinger, F.; Poirier, J. E. *J. Phys. Chem.* **1980**, *84*, 2933.
(20) Bottero, J. Y.; Tchoubar, D.; Cases, J. M.; Fiessinger, F. *J. Phys. Chem.* **1982**, *86*, 3667.
(21) Bottero, J. Y.; Axelos, M.; Tchoubar, D.; Cases, J. M.; Fripiat, J. J.; Fiessinger, F. *J. Colloid Interface Sci.* **1987**, *117*, 47.
(22) Bradley, S. M.; Kydd, R. A.; Yamdagni, R. *J. Chem. Soc., Dalton Trans.* **1990**, 413.
(23) Bradley, S. M.; Kydd, R. A.; Yamdagni, R. *J. Chem. Soc., Dalton Trans.* **1990**, 2653.
(24) Bradley, S. M.; Kydd, R. A. *J. Chem. Soc., Dalton Trans.* **1993**, 2407.
(25) Bradley, S. M.; Kydd, R. A. *J. Catal.* **1993**, *141*, 239.
(26) Bradley, S. M.; Kydd, R. A. *J. Catal.* **1993**, *142*, 448.
(27) Gonzalez, F.; Pesquera, C.; Blanco, C.; Benito, I.; Mendioroz, S. *Inorg. Chem.* **1992**, *31*, 727.
(28) Hernando, M. J.; Pesquera, C.; Blanco, C.; Benito, I.; Mendioroz, S. *Chem. Mater.* **1996**, *8*, 76.

likeliness of the existence of a Ga_{13} polycation. Recently,[29,30] Ga EXAFS measurements of hydrolyzed $GaCl_3$ solutions and of gallium intercalated clays revealed that the spectra in both cases could be modeled, assuming a Ga_{13} structure strictly analogous to the Al_{13} Keggin structure. It is also worth noting that a $GaAl_{12}$ polycation where gallium is the central tetrahedral atom has clearly been evidenced when mixed Ga/Al solutions are base-hydrolyzed.[26,31,32]

Much debate has been going on for a few years regarding the formation mechanism of such Keggin structures, the main problem being the reaction pathway by which octahedral atoms can evolve toward a tetrahedral coordination in the polycation. Several authors[33−36] assume that tetrahedral aluminum $Al(OH)_4^-$ is needed as a precursor for the formation of the Al_{13} moiety. Such a tetrahedral monomer would then be formed at the injection point of the base due to the high local hydroxide concentration and be quickly stabilized by surrounding octahedral oligomers. On the other hand, some studies[37] favor a mechanism in which the tetrahedral precursor is not preformed but takes such coordination once an octahedral monomer condenses with four surrounding planar trimers to form the 13-atom unit. This latter reaction pathway is supported by calculations using the partial charge model[2−4] the recent development of which has provided a useful theoretical guideline for predicting the most probable reaction intermediates along the pathway of hydrolysis of metal cations. Whatever the favored mechanism, they all assume the presence of oligomeric precursors the structures of which remain largely unknown. The only species evidenced are an edge-linked dimer (observed by X-ray diffraction after precipitating partially hydrolyzed solutions by sulfate anions[13]) and trimers of an unknown structure (detected by potentiometric titration[38] and ^{27}Al NMR[18]). There is then a definite need for a better analysis of the oligomeric species involved in the formation of the Keggin-type polycations.

In most studies dealing with aluminum and gallium base hydrolysis, solution NMR was the chosen spectroscopic method. Indeed, such a technique is very sensitive to changes in the coordination of the investigated nucleus and has provided unequivocal evidence for the existence of the polycationic structure.[15−20] Unfortunately, due to their nuclear properties, both gallium and aluminum exhibit rather broad NMR resonances, and this prevents the assignment of the octahedral signal to various oligomeric species. On the other hand, as shown by recent studies on the hydrolytic chemistry of iron[39−42] chromium,[43,44] lanthanum,[45] titanium,[46]..., extended X-ray absorption
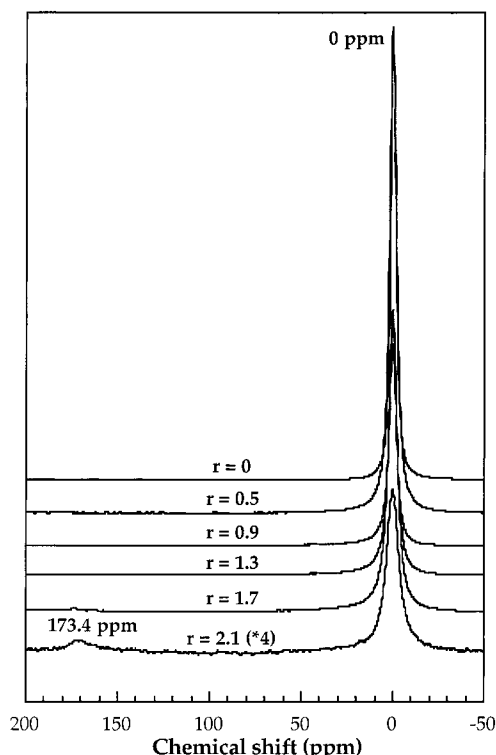

Figure 1. Evolution of ^{71}Ga NMR spectrum of gallium chloride with the hydrolysis ratio $r = OH/Ga$.

fine structure (EXAFS) spectroscopy is extremely well-suited to analyze the nature of species in solution and their evolution upon the first hydrolysis stages but is much less sensitive to changes in the coordination of the atom. It is also rather difficult to implement for light atoms such as aluminum. The aim of the present paper is then to combine ^{71}Ga NMR and Ga K-edge EXAFS measurements for unraveling the formation mechanism of the Ga_{13} Keggin polycation upon base hydrolysis of gallium chloride and gallium nitrate.

Materials and Methods

Sample Preparation. Gallium salts used in this study were high purity anhydrous $GaCl_3$ (99.99%+) and hydrated $Ga(NO_3)_3$ (99.99%+ $H_2O \approx 21$ wt %) purchased from Aldrich Chemicals. Stock solutions of 0.6 M gallium salts were obtained by dilution, using ultrapure water (Millipore). Due to the very hygroscopic character of $GaCl_3$ and to the uncertainty in the water content of hydrated $Ga(NO_3)_3$, both solutions were retitrated by atomic absorption spectrometry after the experiments.

As it has been shown in the case of aluminum hydrolysis that the synthesis conditions have a strong influence on the nature and relative concentrations of the formed species,[34,36] hydrolysis reactions for the present study were carried out in carefully controlled conditions. A small polymethacrylate reactor of standard geometry[47] was built. It has the same height ($H = 7.5$ cm) and diameter (D). Four baffles (size $D/10$) are added to minimize vortex formation upon stirring. The solutions were stirred using a rectangular helix (width $D/3$, height $D/10$) turning at 500 rpm located at $H/3$ cms from the bottom. Fifty milliliters

(29) Montargès, E.; Michot, L. J.; Ildefonse, P. *Microporous Mesoporous Mater.* **1999a**, *28*, 83.

(30) Montargès, E.; Michot, L. J.; Ildefonse, P. In *Clays for our Future*; Kodama, H., Mermut, A. R., Torrance, J. K., Eds.; Proceedings of the 11th International Clay Conference: Ottawa, Canada, 1997; pp 451−456.

(31) Bradley, S. M.; Kydd, R. A.; Fyfe, C. A. *Inorg. Chem.* **1992**, *31*, 1181.

(32) Parker, W. O.; Millini, R.; Kiricsi, I. *Inorg. Chem.* **1997**, *36*, 571.

(33) Bertsch, P. M. *Soil Sci. Soc. Am. J.* **1987**, *51*, 825.

(34) Kloprogge, J. T.; Seykens, D.; Jansen, J. B. H.; Geus, J. W. *J. Non-Cryst. Solids* **1992**, *142*, 94.

(35) Kloprogge, J. T.; Seykens, D.; Jansen, J. B. H.; Geus, J. W. *J. Non-Cryst. Solids* **1993**, *160*, 144.

(36) Morgado, E., Jr.; Lam, Y. L.; Nazar, L. F. *J. Colloid Interface Sci.* **1997**, *188*, 257.

(37) Brinker, C. J.; Scherer, G. W. *Sol-Gel Science: The Physics and Chemistry of Sol-Gel Processing*; Academic Press: San Diego, 1990.

(38) Brown, P. L.; Sylva, R. N.; Batley, G. E.; Ellis, J. *J. Chem. Soc., Dalton Trans.* **1985**, 1967.

(39) Bottero, J. Y.; Manceau, A.; Villiéras, F.; Tchoubar, D. *Langmuir* **1994**, *10*, 316.

(40) Rose, J.; Manceau, A.; Bottero, J. Y.; Masion, A.; Garcia, F. *Langmuir* **1996**, *12*, 6701.

(41) Rose, J.; Flank, A. M.; Masion, A.; Bottero, J. Y.; Elmerich, P. *Langmuir* **1997**, *13*, 1827.

(42) Rose, J.; Manceau, A.; Masion, A.; Bottero, J. Y. *Langmuir* **1997**, *13*, 3240.

(43) Jones, D. J.; Rozière, J.; Maireles-Torres, P.; Jimenez-Lopez, A.; Olivera-Pastor, P.; Rodriguez-Castellon, E.; Tomlinson, A. A. G. *Inorg. Chem.* **1995**, *34*, 4611.

(44) Roussel, H.; Briois, V.; Elkaïm, E.; Dexpert, H.; De Roy, A.; Besse, J. P. *Chem. Mater.*, manuscript submitted.

(45) Ali, F.; Chadwick, A. V.; Smith, M. E. *J. Mater. Chem.* **1997**, *7*, 285.

(46) Chemseddine, A.; Moritz, T. *Eur. J. Inorg. Chem.* **1999**, *2*, 235.

(47) Holland, F. A.; Chapman, F. S. *Liquid Mixing and Processing in Stirred Tanks*; Rheinhold Publishing: New York, 1966.
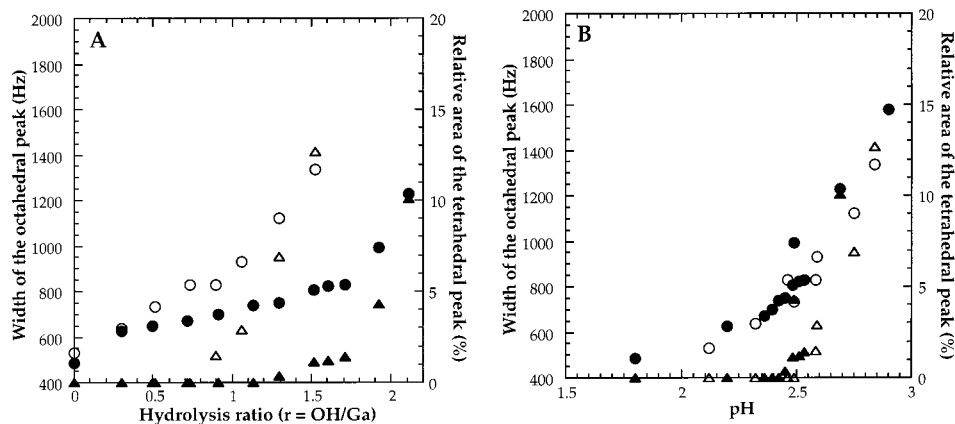
Figure 2. Evolution of the width of the octahedral peak (○) and of the relative area of the tetrahedral signal (△) with **A**: $r = OH/Ga$, **B**: pH. Open symbols $Ga(NO_3)_3$, Filled symbols: $GaCl_3$.

of a sodium hydroxide (Normapur Prolabo) solution at various concentrations was added to 50 mL of the stirred gallium solution at a rate of 50 mL/hour using a syringe pump (Harvard Apparatus type 22). After base addition the solution was stirred for an additional 45 min before collection for further analysis. The pH was recorded after each run in order to draw a rough titration curve. The amount of sodium hydroxide actually added in the reaction tank was controlled by weighing the syringes before and after addition.

NMR Experiments. Nuclear magnetic resonance experiments were performed on a Bruker ASX500 spectrometer at 11.7 T. To perform quantitative measurements, weighted amounts of solution were placed in a 5 mm diameter glass tube of 1 cm length occupying only the middle part of the rf coil of a Bruker static probe with a high quality factor. ^{71}Ga one-pulse experiments were performed with a $\pi/4$ pulse duration of 1.7 μs and a recycle time of 1 s. Between 2000 and 8000 acquisitions were performed depending on the intensity of the signal. A line broadening of 100 Hz was applied, and the spectra were referenced to a 1 M aqueous solution of $Ga(NO_3)_3$. The resulting NMR spectra were fitted using pure Lorentzian curves.

EXAFS Measurements. EXAFS measurements were carried out at the Laboratoire pour l'Utilisation du Rayonnement Electromagnétique (LURE, Orsay, France) on the D44 station of the DCI storage ring (1.85 GeV and 300 mA). The X-rays were monochromatized using a Si(111) double crystal and detected by using ionization chambers filled with a mixture of argon and air. X-ray absorption spectra were recorded in transmission at room temperature and ambient pressure around the Ga K edge (10367 eV) from 10250 to 11240 eV with 2 eV steps and 2 s collecting time. In the range of hydrolysis ratios investigated, all samples can be studied in solution. A special cell[48] with an adjustable path length was then used. Using such device was the best compromise, taking into account the background absorption of the solvent. A good signal/noise ratio can then be easily obtained.

As described elsewhere,[29,30] EXAFS data were reduced using standard procedures[49] with software written by Michalowicz.[50,51] A Kaiser window (3.5−14.7 Å^{-1}) was used for deriving Fourier transforms from EXAFS spectra. The radial distribution functions (RDFs) obtained are not corrected for phase shifts, which leads to peaks shifted down by ∼0.3 Å compared with crystallographic distances.

For modeling experimental spectra, theoretical phase shifts and amplitude backscattering functions were calculated from the α-GaOOH structural model using FEFF 6 code that takes into account the spherical-wave nature of the ejected photoelectron as well as multiple-scattering
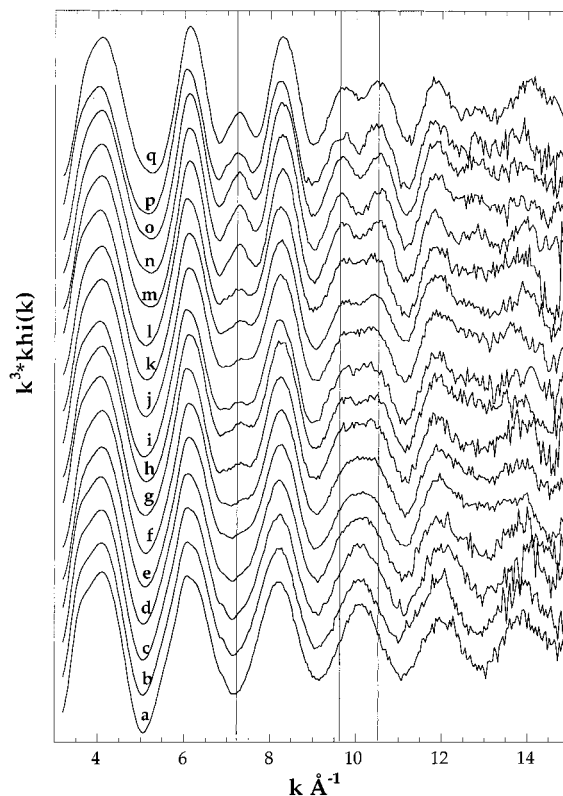
(48) Villain, F.; Briois, V.; Castro, I.; Helary, C.; Verdaguer, M. *Anal. Chem.* **1993**, *65*, 2545.

(49) Teo, B. K. *EXAFS: Basic principles and data analysis*, Inorganic Chemistry Concepts Series; Springer-Verlag: New York, 1986; Vol. 9.

(50) Michalowicz, A. Methods and Softwares for X-ray Absorption Spectra Analysis. Applications for Studying Local Order and Crystalline Disorder in Inorganic Materials. [Méthodes et programmes d'analyse des spectres d'absorption des rayons X (EXAFS). Applications à l'étude de l'ordre local et du désordre cristallin dans les matériaux inorganiques.] Ph.D. Thesis, Université Paris Val de Marne, 1990; pp 211−241.

(51) Michalowicz, A. *Soc. Fr. Chim.* **1991**, 102.

Figure 3. Ga $k^3 \chi(k)$ spectra for gallium chloride solutions at various hydrolysis ratios $r = OH/Ga$: **a**: $r = 0$, **b**: $r = 0.3$, **c**: $r = 0.5$, **d**: $r = 0.7$, **e**: $r = 0.8$, **f**: $r = 0.9$, **g**: r = 1 0.0, **h**: $r = 1.1$, **i**: $r = 1.2$, **j**: $r = 1.3$, **k**: $r = 1.4$, **l**: $r = 1.5$, **m**: $r = 1.6$, **n**: $r = 1.7$, **o**: $r = 1.8$, **p**: $r = 2.0$, **q**: $r = 2.2$.

contributions.[52] The elastic electron mean free path ($\lambda = k/\Gamma$) was determined from α-GaOOH and was kept constant for all samples ($\Gamma = 0.16$ for Ga−O shell and $\Gamma = 0.38$ for Ga−Ga shells). The global scale factor S_0, which is a many-body amplitude reduction factor, was fixed at 0.7 as preconised by Teo.[49] Numbers and distances of nearest neighbors were derived from least-squares fitting. Fitting was first carried out on individual contributions (oxygen neighbors shell and gallium neighbor shells), and parameters were finally refined on the complete spectrum. According to classically admitted values,[49] the accuracy on distances is taken as ±0.01 Å, and the accuracy on Debye−Waller factors and number of neighbors as ±10%.

Results

^{71}Ga NMR Experiments. ^{71}Ga NMR spectra obtained for selected hydrolysis ratios of gallium chloride are presented in

(52) Mustre, J.; Rehr, J. J.; Zabinsky S. I.; Albers, R. C. *Phys. Rev. B* **1991**, *44*, 4146.

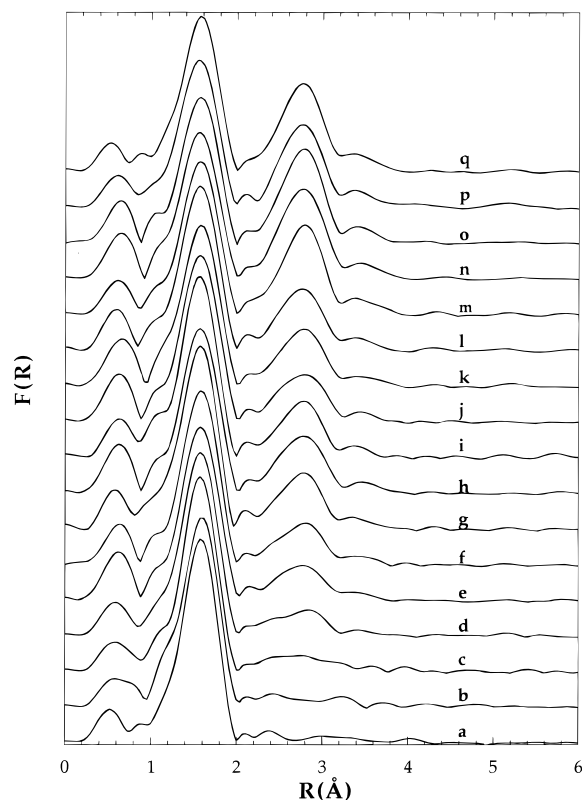**Figure 4.** Gallium RDFs (uncorrected for phase shifts) for gallium chloride solutions at various hydrolysis ratios $r = OH/Ga$: **a**: $r = 0$, **b**: $r = 0.3$, **c**: $r = 0.5$, **d**: $r = 0.7$, **e**: $r = 0.8$, **f**: $r = 0.9$, **g**: $r = 1.0$, **h**: $r = 1.1$, **i**: $r = 1.2$, **j**: $r = 1.3$, **k**: $r = 1.4$, **l**: $r = 1.5$, **m**: $r = 1.6$, **n**: $r = 1.7$, **o**: $r = 1.8$, **p**: $r = 2.0$, **q**: $r = 2.2$.

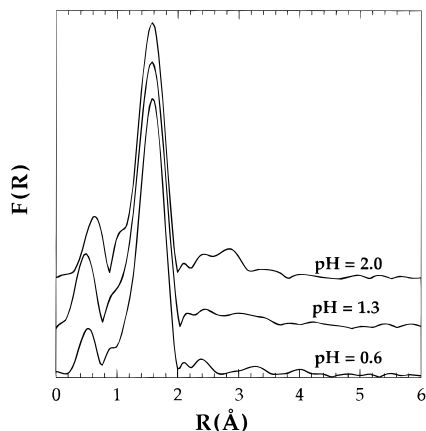**Figure 5.** Evolution with pH of the gallium RDFs (uncorrected for phase shifts) for gallium nitrate solutions at a hydrolysis ratio $r = OH/Ga = 0$.

Table 1: Structural Parameters for the Second Coordination Sphere of Gallium Atoms Derived from the EXAFS Analysis of Gallium Chloride at Increasing Hydrolysis Ratios $r = OH/Ga$

r OH/Ga	$R_1{}^a$	$N_1{}^b$	$\sigma_1{}^c$	$R_2{}^a$	$N_2{}^b$	$\sigma_2{}^c$	$R_3{}^a$	$N_3{}^b$	$\sigma_3{}^c$	Q^d
0	3.05	0.27	0.077	-	-	-	-	-	-	0.0135
0.3	3.01	0.37	0.071	3.43	0.17	0.069	-	-	-	0.0160
0.5	3.03	0.45	0.070	3.47	0.32	0.07	3.91	0.13	0.06	0.0146
0.7	3.05	0.86	0.076	3.51	0.30	0.085	3.95	0.20	0.090	0.0134
0.8	3.04	1.27	0.082	3.50	0.58	0.092	3.90	0.18	0.075	0.0147
0.9	3.04	1.72	0.088	3.52	0.55	0.100	3.89	0.25	0.080	0.0154
1.0	3.04	1.80	0.081	3.52	0.82	0.095	3.91	0.45	0.100	0.0165
1.1	3.04	1.90	0.081	3.52	0.85	0.104	3.91	0.60	0.105	0.0086
1.2	3.05	1.80	0.081	3.54	0.85	0.098	3.91	0.40	0.115	0.0127
1.3	3.050	1.65	0.085	3.55	0.65	0.102	3.90	0.45	0.104	0.0131
1.4	3.050	2.02	0.083	3.52	0.90	0.104	3.92	0.52	0.103	0.0114
1.5	3.05	2.07	0.081	3.53	0.95	0.095	3.89	0.42	0.103	0.0103
1.6	3.050	2.55	0.076	3.53	1.54	0.105	3.92	0.30	0.080	0.0092
1.7	3.05	2.62	0.074	3.52	1.61	0.104	3.92	0.32	0.070	0.0139
1.8	3.08	2.59	0.075	3.54	1.66	0.102	3.90	0.15	0.060	0.0170
2.0	3.05	2.52	0.078	3.53	1.60	0.101	3.91	0.15	0.052	0.0103
2.2	3.05	2.77	0.080	3.53	1.85	0.102	-	-	-	0.0277

^{a} R_i is the distance between two atoms of each atomic pair. ^{b} N_i is the number of atoms at distance R_i. ^{c} σ_i is the Debye−Waller factor (Å) for subshell i. ^{d} $Q = \Sigma[(k^3\chi_{calc}) - (k^3\chi_{exp})]^2/\Sigma(k^3\chi_{exp})^2$.

Table 2: Structural Parameters for the Second Coordination Sphere of Gallium Atoms Derived from the EXAFS Analysis of Gallium Nitrate at Increasing Hydrolysis Ratios $r = OH/Ga$

r = OH/Ga	$R_1{}^a$	$N_1{}^b$	$\sigma_1{}^c$	$R_2{}^a$	$N_2{}^b$	$\sigma_2{}^c$	$R_3{}^a$	$N_3{}^b$	$\sigma_3{}^c$	Q^d
0 pH 0.6	-	-	-	-	-	-	-	-	-	0.0105
0 pH 1.5	3.05	0.40	0.082	3.50	0.30	0.072	-	-	-	0.0137
0 pH 2.1	3.05	0.65	0.075	3.52	0.33	0.080	-	-	-	0.0215
0.3	3.04	0.90	0.078	3.51	0.70	0.088	-	-	-	0.0184
0.5	3.05	1.45	0.081	3.51	0.62	0.105	3.90	0.35	0.097	0.0071
0.7	3.05	1.65	0.078	3.51	0.78	0.097	3.93	0.30	0.102	0.0081
0.9	3.05	1.85	0.078	3.52	0.85	0.095	3.91	0.50	0.100	0.0142
1.0	3.05	1.80	0.075	3.51	0.95	0.095	3.91	0.55	0.098	0.0113
1.2	3.05	2.07	0.070	3.51	1.02	0.102	3.95	0.36	0.068	0.0058
1.3	3.05	2.35	0.074	3.54	1.30	0.103	3.92	0.50	0.105	0.0092
1.4	3.05	2.34	0.071	3.51	1.46	0.105	3.96	0.42	0.081	0.0047
1.5	3.05	2.35	0.078	3.53	1.40	0.104	3.94	0.27	0.084	0.0091
1.6	3.05	2.50	0.081	3.53	1.52	0.106	3.94	0.25	0.075	0.0084
1.7	3.05	2.70	0.079	3.53	1.74	0.111	3.90	0.12	0.051	0.0104

^{a} R_i is the distance between two atoms of each atomic pair. ^{b} N_i is the number of atoms at distance R_i. ^{c} σ_i is the Debye−Waller factor (Å) for subshell i. ^{d} $Q = \Sigma[(k^3\chi_{calc}) - (k^3\chi_{exp})]^2/\Sigma(k^3\chi_{exp})^2$.

Figure 1, whereas Figure 2 presents the evolution of various parameters derived from the NMR spectra for both gallium chloride and gallium nitrate. In the case of the chloride salt, for low hydrolysis ratios ($r < 1.3$) a single peak corresponding to octahedral gallium is observed at 0 ppm. (Figure 1). For $r = 0$ the peak width is around 450 Hz for chloride ions and around 600 Hz for nitrate ions (Figure 2A). Both values are indicative of already partially hydrolyzed species as acidified gallium perchlorate solutions at low concentrations exhibit a peak width of $\approx$ 50 Hz.[53] As hydrolysis progresses, this octahedral peak broadens, but as already observed,[23,24,53] no shift in position can be noticed. For $r \geq 1.3$, a small broad peak located around 172 ppm appears. It is barely visible for $r = 1.3$ and increases

then relative to the octahedral peak at 0 ppm to reach around 10% around $r = 2.1$ (Figure 2A). This peak corresponds to gallium atoms in a distorted tetrahedral environment and has previously been assigned to the central gallium atom of a $[GaO_4\text{-}Ga_{12}(OH)_{24}(H_2O)_{12}]^{7+}$ (Ga_{13}) polycation.[22,23] In the case of gallium nitrate (spectra not shown), this peak appears for a hydrolysis ratio of 0.9 and then follows the same evolution as in the case of gallium chloride. This discrepancy in r values seems to be due to the shift in pH between gallium chloride and gallium nitrate stock solutions. Indeed, when the data of Figure 2A are replotted as a function of solution pH rather than as a function of r (Figure 2B), they are nearly superimposed for both anions.

EXAFS experiments. Figure 3 presents the evolution of the EXAFS spectra with increasing hydrolysis for gallium chloride. The data obtained for nitrate samples are similar and are therefore not presented. Scans were performed over a high energy range, and EXAFS data can be extracted up to $k = 14.3$ Å^{-1} which fixes the distance resolution ΔR at $\sim$0.1 Å according to the formula $\Delta R = \pi/2k$.[49]

Obvious changes can be observed around $k = 7.2$, 9.7, and 10.5 Å^{-1} where new resonances appear and grow upon

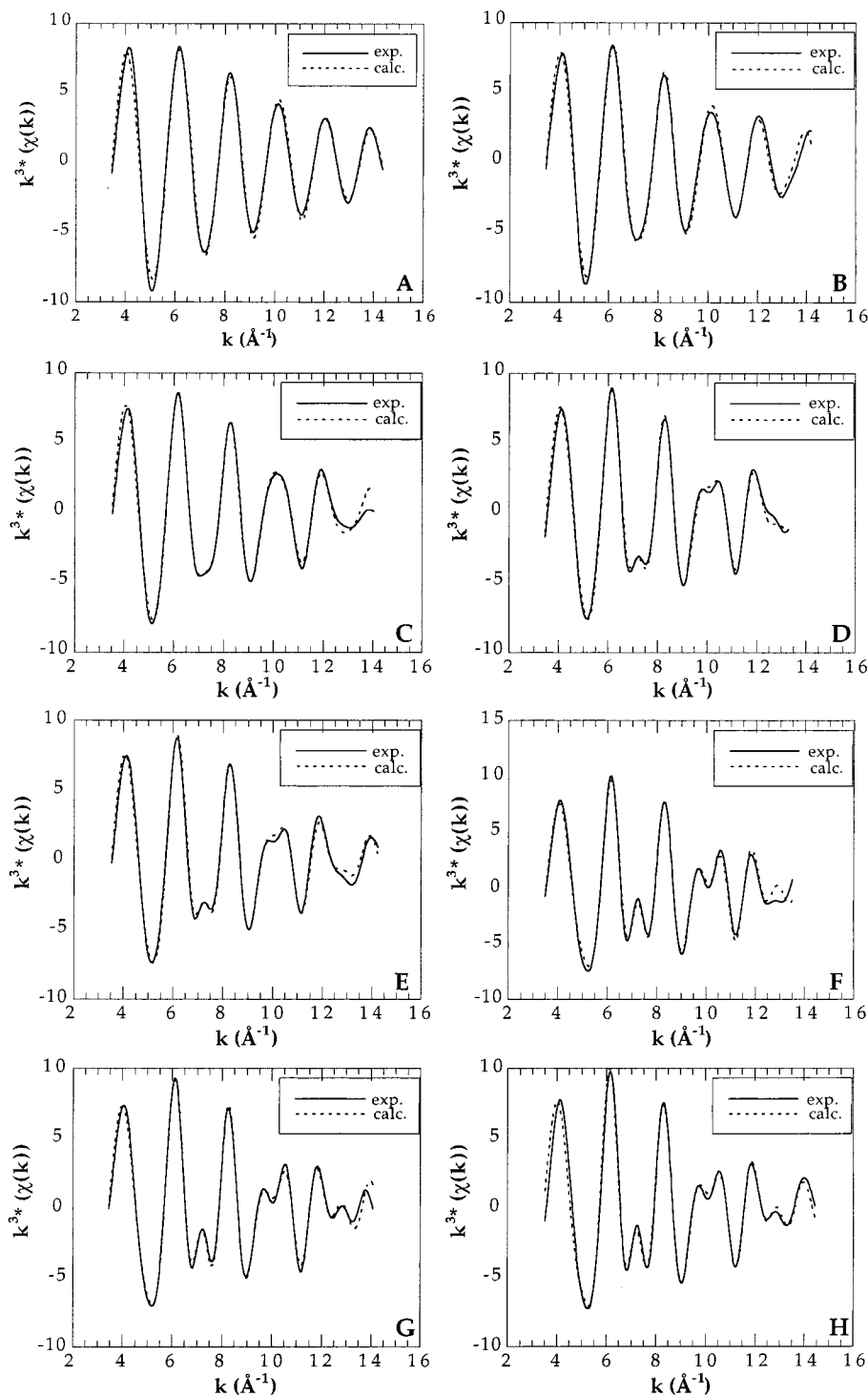(53) Akitt, J. W.; Kettle, D. *Magn. Reson. Chem.* **1989**, *27*, 377.

Figure 6. Filtered EXAFS spectra of gallium chloride solutions at various *r* values. Solid line: experimental spectrum. Dotted line: calculated spectrum. **A**: *r* = 0, **B**: *r* = 0.5, **C**: *r* = 0.8, **D**: *r* = 1.1, **E**: *r* = 1.4, **F**: *r* = 1.7, **G**: *r* = 2.0, **H**: *r* = 2.2.

increasing hydrolysis. These changes in the EXAFS spectra are very strongly revealed in the radial distribution functions (RDFs) (uncorrected for phase shifts) presented in Figure 4. The first peak corresponds to oxygen neighbors and changes very little with increasing hydrolysis ratio. A set of peaks at higher distances that can be assigned mainly to gallium–gallium contributions grows as hydrolysis progresses.

When no base is added, it is observed, as already revealed by [71]Ga NMR experiments, that gallium nitrate is more hydrolyzed than gallium chloride. Therefore, the peaks observed at distances >2.5 Å for non-hydrolyzed gallium nitrate (Figure 5) should be assigned to Ga–Ga contributions and not to the

second hydration shell as proposed in a recent publication.[54] To prove this point unambiguously, we collected the Ga EXAFS spectra of 0.3 M gallium nitrate after acidifying the solutions with 1 M nitric acid. As shown in Figure 5, when the pH is lowered, the higher distances contribution decrease and even nearly disappears for a pH of 0.6.

Discussion

EXAFS Modeling: Analysis of Ga Binding Environments. 1. First Coordination Shell. Results obtained from modeling of the first coordination sphere show that for hydrolysis ratios ≤1.8 for chloride and ≤1.4 for nitrate, the first coordination
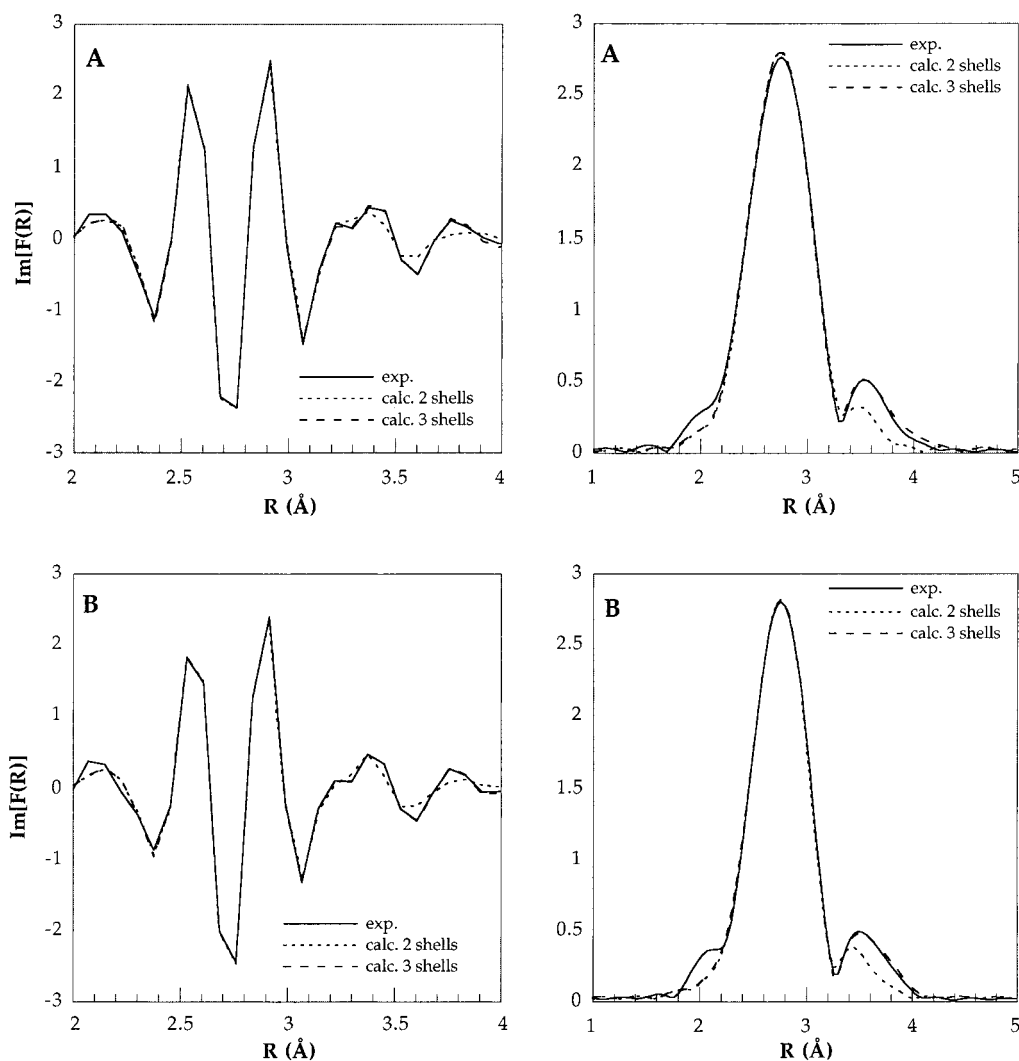
Figure 7. Comparison between experimental imaginary parts (left) and RDFs (right) and calculated data assuming two or three subshells of gallium atoms. **A**: GaCl₃ $r = 1.1$, **B**: GaCl₃ $r = 1.4$.

shell is formed of six oxygen atoms located at 1.95 ± 0.01 Å from the central gallium atom in agreement with previous findings.[54,55] For both salts, at the higher end of investigated r values (1.5 to 1.7 for nitrate and 2.0 and 2.2 for chloride), better modeling results are obtained by splitting the six oxygen neighbors into four neighbors at 1.92 ± 0.01 Å and two neighbors at 2.03 ± 0.01 Å. This difference in distance is of the order of the resolution distance, and the separation of the first shell into two sub-shells is then debatable. However, this two-shell modeling, which appears necessary for maximal concentrations of Ga₁₃ species in solution, fits the reported structure of Al₁₃ sulfates crystals.[11−14] Indeed, each aluminum octahedron in the Al₁₃ structure has the formula [AlO(OH)₄-(H₂O)]. Thus, its first neighbor shell consists of four hydroxyl groups at a mean distance of 1.85 Å, one oxygen atom at 2.03 Å (shared with the central tetrahedron), and one water group at 1.95 Å. Taking into account the differences in ionic radii between gallium and aluminum in octahedral coordination (0.62 and 0.53 Å, respectively), the two Ga−O distances obtained in our simulation, 1.92 ± 0.01 Å and 2.03 ± 0.01 Å could then

be tentatively assigned to Ga−OH for short distances and to Ga−O and Ga−H₂O for large distances.

2. Analysis of the Second Coordination Shell. (a) Ga−Ga Distances. Tables 1 and 2 show the best fit structural parameters obtained in the modeling of the second coordination shell of gallium atoms for chloride and nitrate salts, respectively. The results presented correspond to the fit of the complete Fourier back-transform of the RDFs in the range 0.8−4.1 Å. The fit of the first coordination shell did not need any refinement, and for the second coordination shell, the distances, number of neighbors, and Debye−Waller factor values were freed. As an illustration, Figure 6 shows comparisons between experimental and calculated curves for gallium chloride at some selected values of the hydrolysis ratio $r = $ OH/Ga. As revealed by the curves and by the Q values displayed in Tables 1 and 2, the agreement between experimental and calculated values is excellent.

For both chloride and nitrate, the values obtained suggest the presence of three atomic shells of gallium neighbors:

a first shell Ga−Ga₁ at 3.01−3.05 Å

a second one Ga−Ga₂ at 3.47−3.53 Å

a third one Ga−Ga₃ at 3.90−3.95 Å

(54) Muñoz-Páez, A.; Diaz-Moreno, S.; Sánchez-Marcos, E.; Martinez, J. M.; Pappalardo, R. R.; Persson, I.; Sandström, M.; Pattanaik, S.; Lindqvist-Reis, P. *J. Phys. Fr.* **1997**, *7*, C2−647.

(55) Lindqvist-Reis, P.; Muñoz-Páez, A.; Diaz-Moreno, S.; Pattanaik, S.; Persson, I.; Sandström, M. *Inorg. Chem.* **1998**, *37*, 6675.
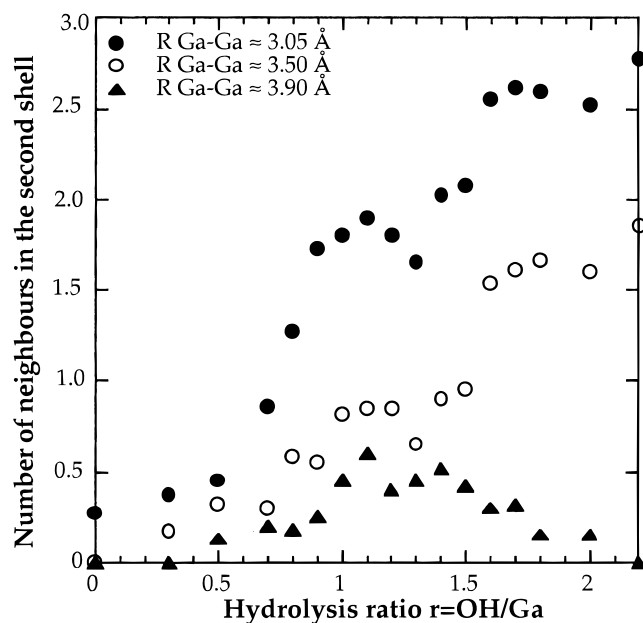
Figure 8. Evolution of the number of gallium neighbors in the different subshells of hydrolyzed gallium chloride as a function of the hydrolysis ratio r = OH/Ga.

The first distance corresponds to edge-sharing gallium octahedra as it is close to the values obtained in various gallium compounds with edge-sharing octahedra: d Ga−Ga $\approx$ 2.97 Å in α-GaOOH,[56] d Ga−Ga = 3.04−3.20 Å in β-Ga$_2$O$_3$.[57] By contrast, face-sharing octahedra would lead to much shorter distances: d Ga−Ga = 2.835 Å in α-Ga$_2$O$_3$.[58]

The second distance around 3.5 Å could be related to various structural models. It could be assigned to single corner-sharing between a gallium tetrahedron and a gallium octahedron. Indeed, such a ^{IV}Ga−^{VI}Ga distance in β-Ga$_2$O$_3$ is equal to 3.45 Å.[57] Furthermore in the Al$_{13}$ sulfate crystal structures,[11−14] the crystallographic distances are ^{VI}Al−^{VI}Al = 2.94 Å and ^{IV}Al−

^{VI}Al = 3.41 Å. However, this distance is already observed for low hydrolysis ratios where ^{71}Ga NMR experiments preclude the presence of tetrahedral gallium. In this case, it must then be assigned to double corner sharing gallium octahedra as a distance ^{VI}Ga−^{VI}Ga = 3.39 Å was reported for α-GaOOH.[56]

The existence of the higher distance contribution Ga−Ga$_3$ at R =3.9−3.95 Å can be questioned for two main reasons: (i) it does not seem to be related to any distinct peak in the RDF (Figure 4), and (ii) the determination of neighbors at distances larger than 3.8 Å where the signal/noise ratio decreases rapidly can be debated. However, based on the quality of the experimental data obtained and the constant distance value of this contribution, it seems reasonable to assume that it is real. Furthermore the addition of this contribution significantly improves the quality of the fits of both the EXAFS and RDF curves.

This is particularly striking, in the range where the number of N$_3$ neighbors is significant when comparing the imaginary parts of the Fourier transforms corresponding to the experimental data (obtained by Fourier back-transform of the 2−4 Å range of the RDF) with those obtained from calculated spectra taking into account two or three gallium subshells (Figure 7 left). It appears that the 3.5−4 Å range is described correctly only by adding the 3.9 Å Ga−Ga distance. The same trend is clearly observed when comparing the corresponding RDFs with those obtained from calculated spectra taking into account two or three gallium subshells (Figure 7 right). The second peak of the RDF can be correctly reproduced only by taking into account the 3.9 Å Ga−Ga distance.

This contribution then appears to really be present and could be assigned to single corner-sharing gallium octahedra. It could, however, also be due to multiple scattering effects, as will be discussed later.

(b) Number of Gallium Neighbors. Figure 8 shows the evolution of the number of neighbors corresponding to these three distances as a function of the hydrolysis ratio for gallium chloride. The evolution is parallel for gallium nitrate (not
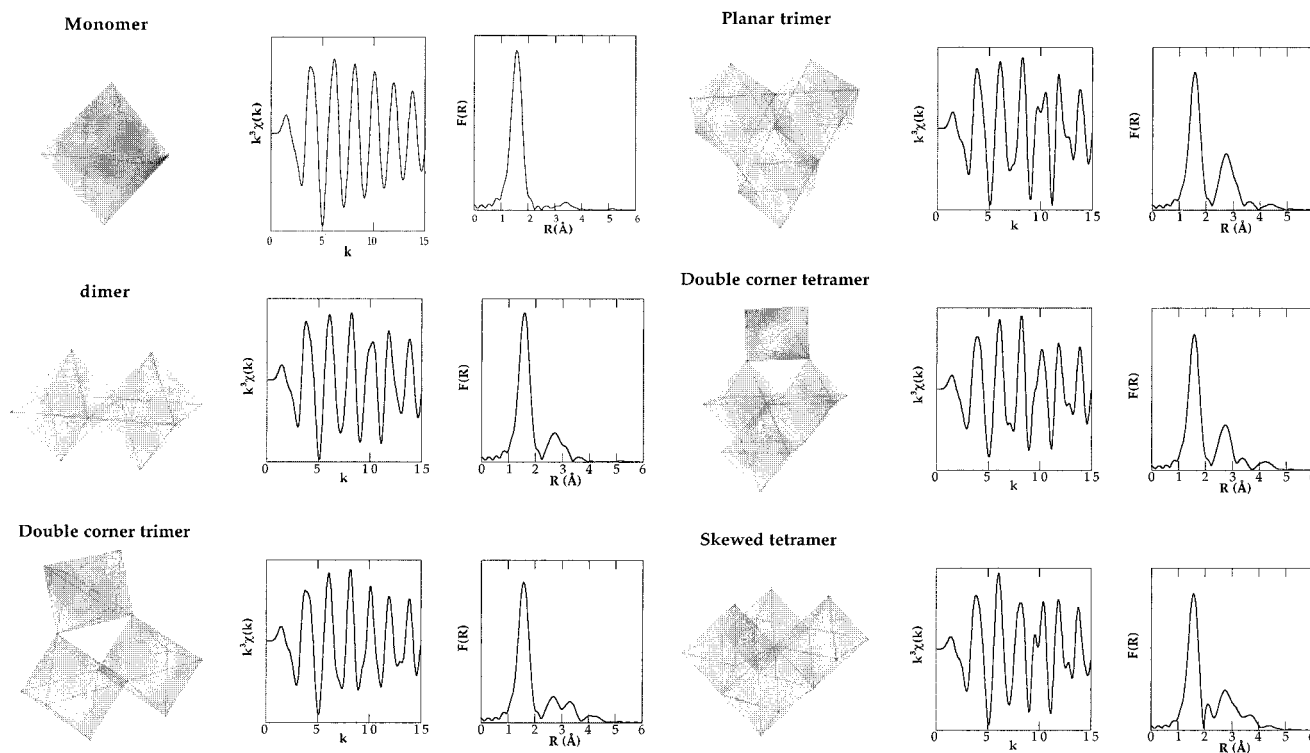

Figure 9. Structure, EXAFS spectra, and RDFs of the various oligomers considered.
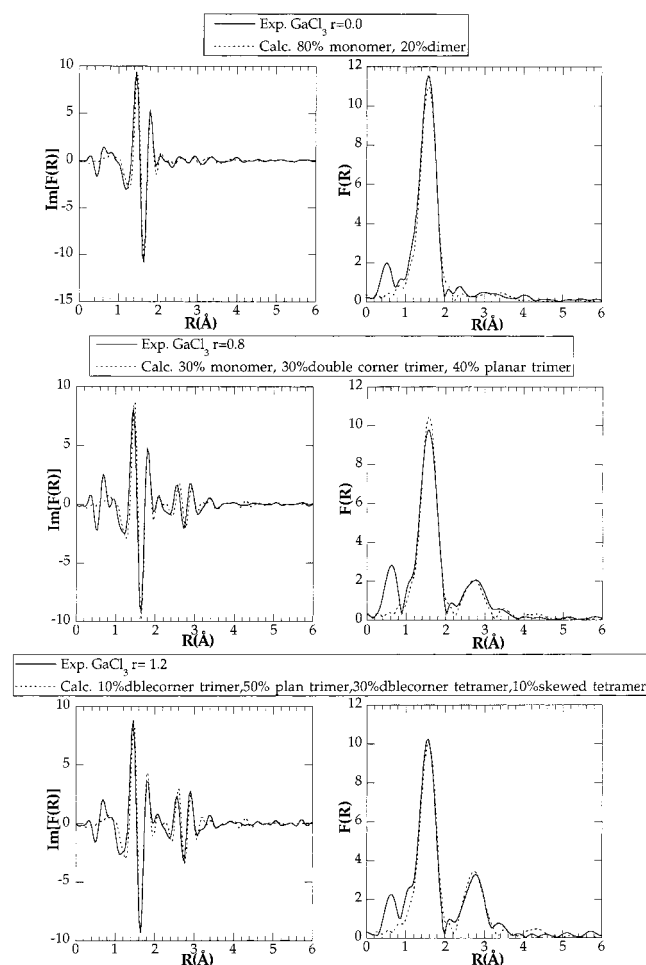
Figure 10. Comparison between experimental imaginary parts (left) and RDFs (right) and calculated data (by the Feff 7.0.2 code) using various proportions of the oligomers of Figure 9.

Figure 11. Evolution of the proportion of oligomers in a GaCl₃ solution as a function of the hydrolysis ratio $r = OH/Ga$.

1.85 ($1.85 = 1*12/13 + 12*1/13$) for the Ga−Ga contribution at 3.5 Å. Accordingly, the mean numbers of gallium neighbors in such structure must be taken as 2.77 ($3*12/13$) for the gallium−gallium contribution at 3.04 Å. Using those numbers, an excellent fit between calculated and experimental data can be obtained (Table 1 and Figure 6H). This suggests that for a total gallium concentration of 0.3 M, at a hydrolysis ratio $r = OH/Ga = 2.2$, nearly 100% of gallium atoms in the chloride solution are present as the Ga₁₃ polycation. This is certainly also the case for a gallium nitrate solution for $r = 1.7$ (Table 2). [71]Ga NMR experiments also lead to the same conclusion as the octahedral/tetrahedral ratio in these ranges is close to 12 (Figure 2).

Modeling of the Hydrolysis Pathway. Ga₁₃ Formation Mechanism. According to the previous analysis, the nature of the oligomeric precursors present in the solution before the formation of Ga₁₃ polycations can be approached from a careful study of the r domain before 1.3 in the case of chloride anions. The high number of gallium neighbors derived from the modeling of EXAFS spectra suggests the early formation of at least trimeric species in the solution. Furthermore, the proposed formation mechanisms for the Ga₁₃ assuming the condensation of monomers (octahedral or tetrahedral) with planar trimers appears to be not correct. Indeed, from $r = 0.5$, the solution obviously contains some oligomers with double corner-sharing as they are the only species which could give rise to a distance around 3.5 Å.

To go further in our analysis and to obtain the nature and relative amounts of soluble species for various hydrolysis ratios, we calculated the EXAFS spectra of various oligomers using the FEFF 7.0.2 code.[59] In a first check of the validity of our approach, such procedure was first carried out for acidified gallium nitrate. In this case, as only octahedral monomers are present in solution, the main multiple scattering contribution results from a doubling of the Ga−O distance at 1.95 Å which gives rise to a signal at 3.90 Å. The comparison between experimental and simulated spectra thus allows estimating the importance of multiple scattering contributions inside gallium octahedra and to choose the proper Debye−Waller factors to be used for the intra-octahedra paths. It appears that a good fit between experimental and simulated data can be obtained by assuming σ values of 0.05 (Ga−O) and 0.06 (Ga−Ga) for single

shown). The number of neighbors at 3.05 Å (edge-sharing octahedra) exhibits two strong increases for $0.6 \leq r \leq 0.9$ and for $1.3 \leq r \leq 1.7$. The number of neighbors at 3.50 Å (double corner sharing octahedra or single corner-sharing between Ga^VI and Ga^IV) increases more or less linearly up to $r = 1.5$ and then increases steeply. The number of neighbors at 3.9 Å increases strongly for $0.9 \leq r \leq 1.1$ remains approximately constant up to $r = 1.4$ and then decreases regularly down to 0 at $r = 2.2$.

The total number of gallium neighbors is quickly greater than two which suggests that the oligomeric species formed are rapidly at least trimeric even in the first hydrolysis stages. The evolution for $r \geq 1.4$ can certainly be assigned to the formation of increasing amounts of the Ga₁₃ polycation as revealed by [71]Ga NMR experiments that showed that this species appears for $r \approx 1.3$ and increases thereafter.

It must be pointed out that for $r = 2.2$ the Ga EXAFS spectra can be simulated by taking into account only this species. Indeed, assuming an analogy with the Al₁₃ polycation, it has been shown[29,30] that the central tetrahedral gallium has to be considered both as a central absorber and as a backscatterer. As a central absorber it "sees" 12 octahedral gallium atoms at ∼3.5 Å and as a backscatterer it "is seen" once by the 12 octahedral gallium, leading to a mean coordination number of
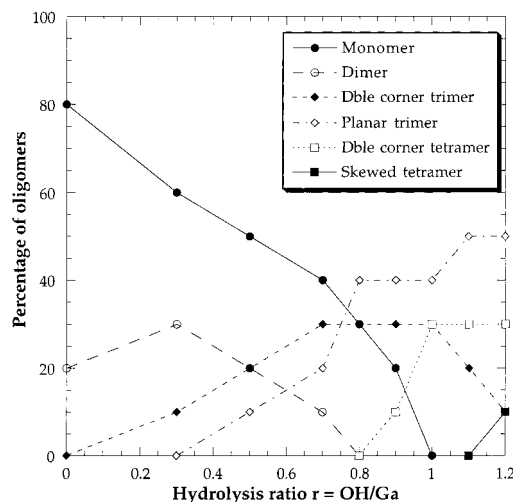
(56) Pye, M. F.; Birtill J. J.; Dickens, P. G. *Acta Crystallogr.* **1977**, *B33*, 3224.

(57) Geller, S. *J. Chem. Phys.* **1960**, *33*, 676.

(58) Marezio, M.; Remeika, J. P. *J. Chem. Phys.* **1967**, *46*, 1862.

(59) Zabinsky, S. I.; Rehr, J. J.; Ankudinov, A.; Albers, R. C.; Eller, M. J. *Phys. Rev. B* **1995**, *52*, 2995.
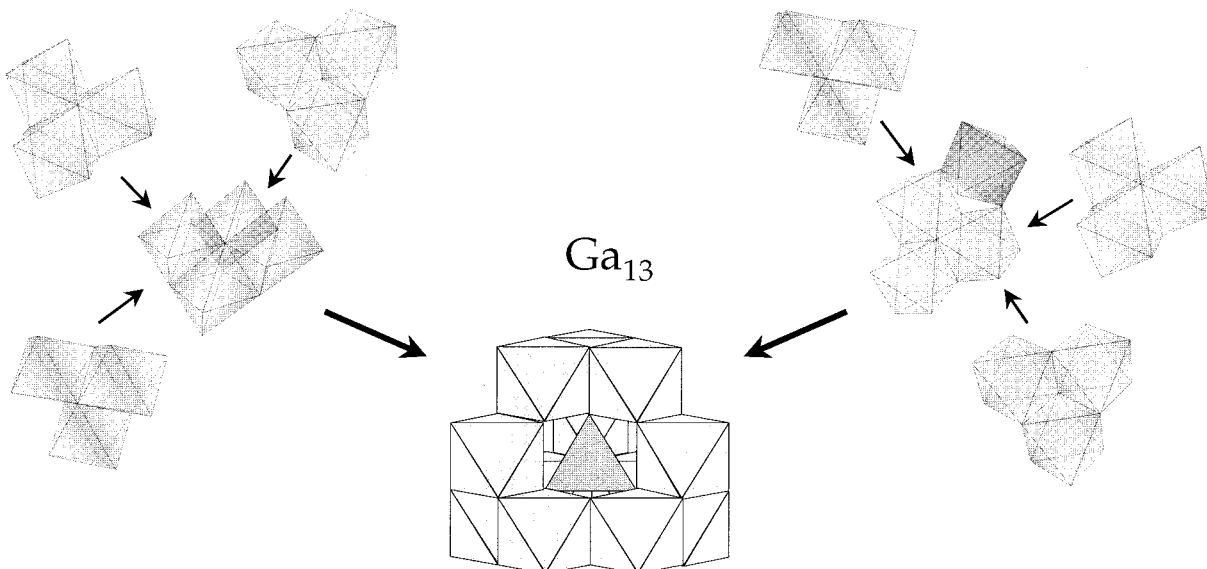
Figure 12. Proposed formation mechanism for the Ga_{13} polycation.

scattering paths, and 0.085 for multiple scattering paths inside the monomer.

The oligomeric species we considered are presented in Figure 9 together with their calculated EXAFS spectra (from FEFF 7.0.2) and the corresponding RDFs. These species were selected on the basis of the distances and number of neighbors previously determined and on literature data. The distance between gallium atoms in adjacent edge-sharing octahedra being around 3.05 Å, the octahedra in the dimer cannot be perfectly symmetrical as shown in Figure 9. The edge-linked dimer was characterized by X-ray crystallography.[13] The double corner trimer has been observed in the case of iron hydrolysis.[4,5,39−42] Such species should exist in the solution in order to explain the distance around 3.50 Å. The planar trimer and the two tetramers have been proposed to play an important role in the hydrolysis of chromium[4,5] and were recently evidenced by Cr K EXAFS measurements.[44] Furthermore, the skewed tetramer has been suggested as the building unit of the boehmite structure.[4,5]

As shown in Figure 10 for some selected r values, all the experimental data for gallium chloride solutions at r values ≤ 1.2 can be reproduced quite satisfactorily by using simple combinations of the six proposed oligomeric species with a logical evolution from the less hydrolyzed (monomers, dimers) to the more hydrolyzed (trimers, tetramers) species (Figure 11). According to these simulations, the following picture could describe the evolution of the species present in hydrolyzed gallium chloride solutions.

For $r = 0$, the solution already contains 20% of edge sharing dimers, which agrees with the NMR data revealing the existence of hydrolyzed species under such conditions. By analogy with the case of aluminum where potentiometric titration[38] and NMR measurements[18] revealed that the dimer is only a minor species, we think that trimers start being present in the solution at very early stages of the hydrolytic pathway (from $r = 0.3$). Two types of trimers could be present: a double corner one, explaining the observed Ga−Ga distance around 3.5 Å and a planar one explaining the strong increase in the number of neighbors at 3.05 Å. For r around 0.9, a double corner tetramer starts appearing which explains the concomitant increase in both the contributions at 3.04 and 3.5 Å. For $r = 1.2$ the solution contains only tetramers and trimers, and further hydrolysis then leads to the formation of a Ga_{13} polycation by association between those species. Upon further hydrolysis, increasing

amounts of Ga_{13} are formed which results in an increase of the contributions at 3.04 and 3.50 Å and a concomitant decrease of those of the other species, revealed by the decrease of the Ga−Ga contribution at 3.9 Å. For $r = 2.0$ nearly all gallium atoms would then be engaged in a Ga_{13} Keggin structure.

In the model we propose, the skewed tetramer forms and nearly immediately associates with planar trimers to form the Ga_{13} polycation. Such tetramer would also explain the distance around 3.9 Å though FEFF simulations reveal that multiple scattering effects (only due to intraoctahedra paths) could be strong enough to explain the spectra in this region. The existence of this skewed tetramer is then not fully evidenced from our experiments and requires further scrutiny. Still, it appears that, in contrast with the available models for the formation of Keggin polycations, the **Ga_{13} polycation is built by direct condensation of three planar trimers with one tetramer** which structure could be either double corner or skewed (Figure 12). Such a scheme does not require the simultaneous presence of non-hydrolyzed and hydrolyzed species and seems then very plausible.

Conclusions

This study shows the potential of the combination of two local spectroscopic techniques, EXAFS and NMR, for understanding hydrolysis/condensation processes in aqueous systems. Indeed, using such experimental methods, we have been able to propose a logical sequence of oligomers leading to the formation of Keggin-type polycations. This work can certainly now be widened to more complex systems such as the hydrolysis of gallium salts in the presence of different organic ligands with increasing complexing power. In view of the analogies observed between the aqueous behavior of aluminum and gallium, such study could provide useful insights about the geocycling of aluminum in natural aqueous environments as well as a better control of aluminum salts based coagulation processes in drinking water treatment operations.